Chinese Chemical Letters 36 (2025) 110083

Contents lists available at ScienceDirect

Chinese Chemical Letters

journal homepage: www.elsevier.com/locate/cclet

Deuterated chloroform replaces ultra-dry chloroform to achieve high-efficient organic solar cells

Zhiyang Zhang, Yi Chen, Yingnan Zhang, Chuanlang Zhan*

Key Laboratory of Advanced Materials Chemistry and Devices (AMCDLab) of the Department of Education of Inner Mongolia Autonomous Region, College of Chemistry and Environment Science, Inner Mongolia Normal University, Huhehot 010022, China

ARTICLE INFO

Article history:
Received 19 March 2024
Revised 31 May 2024
Accepted 2 June 2024
Available online 3 June 2024

Keywords:
Organic solar cell
Processing solvent
Deuterated chloroform
Ultra-dry chloroform
Active layer

ABSTRACT

Chloroform is a common and excellent solvent for preparing high-efficient organic solar cells (OSCs), however, it is toxic and poisonable chemical. In comparisons, deuterated chloroform (DC) is less toxic and costly, and particularly, it is non-poisonable chemical. In this paper, we use DC to replace ultra-dry chloroform (UC) as the processing solvent for preparation of active layers of organic solar cells. First, we selected PM6:BTP-eC9 as the basic binary and counted 100 solar cells' data, from which comparable device performance were obtained with use of DC and UC. Interestingly, DC showed better reproducibility, superior storage under a nitrogen atmosphere and a little better performance than UC. Both DC and UC gave rise of comparable hole and electron mobilities and similar charge recombination losses. Second, we based PM6:Y6 and D18-Cl:Y6 as the binaries and similar effects were obtained from both UC and DC when counting 30 devices for each binary. Third, the universality of the use of DC for preparing high-efficient OSCs were again checked with several binary and ternary systems. In all, this study demonstrate that DC can replace UC for use in the field of OSCs.

Solution-processable organic solar cells (OSCs) are a research priority due to their low cost, light weight, mechanical flexibility, semi-transparency, and roll-to-roll printability [1–9]. The efficiencies of single-junction and tandem OSCs has exceeded 19% and 20%, respectively, indicating that OSCs are approaching commercialization [10–17]. The performance of OSCs is significantly influenced by the photoactive layer [18–20]. Therefore, it is crucial to ensure good solubility of the donor and acceptor materials in the processing solvents to achieve ideal nanoscaled morphology of the donor and acceptor materials. This, in turn, determines molecular crystallinity, domain size, phase separation, and bi-continuous network structure [21–23]. The morphology of the active layer is influenced by six key components that directly impact the solar cell's performance: molecular structure, processing solvent, component ratios, total component concentration, additives, and processing conditions (including dissolution, film formation, and post-film formation) [24]. The solubility of each component must be high enough to produce the active layer morphology and also appropriate blend of film thickness for effective photon capture [25]. To ensure optimal device performance, the processing solvent must dissolve both the donor and acceptor components and promote their phase separation to form a bi-continuous network. Solvents such as chloroform (CF), chlorobenzene (CB), toluene (Tol), and *o*-dichlorobenzene (*o*-DCB) are the solvents that meet these conditions [26–31]. It is important to note that these solvents are mainly halogenated and aromatic [32].

Chloroform is a versatile chemical compound that finds use in various fields such as production, scientific research, and organic synthesis. It serves as a raw material to produce other chemicals, an anesthetic for medical procedures, and a solvent and extractant in various industries. Chloroform is a good solvent to many chemicals and hydrocarbons and ultra-dry chloroform (UC) is a commonly used and excellent solvent in the processing of high-performance OSCs [13,14,33]. Especially, highly efficient Y-series based OSCs are produced with UC the processing solvent. However, the use of UC as a common solvent in the laboratory has several limitations. Firstly, UC is classified as a Class II hazardous chemical, and its purchase is largely restricted. Secondly, UC deteriorates easily upon storage while it is not available in small packages (less than 1 mL), which generally result in deteriorated device's performance. Thirdly, UC is toxic to the human body, which is not conducive to human health. Therefore, it is of significant scientific and practical importance to find a processing solvent that is readily available, non-degradable, less toxic,

* Corresponding author.
E-mail address: clzhan@imnu.edu.cn (C. Zhan).

https://doi.org/10.1016/j.cclet.2024.110083
1001-8417/

and can achieve comparable performance to ultra-dry chloroform devices.

Deuteration is widely used in laboratory research in many fields. For example, Hwang *et al.* applied deuteration in organic light-emitting diodes (OLEDs) by replacing the unstable C–H bonds in the main body with C-D bonds, which increased the device lifetime by a factor of 5 without loss of efficiency and improved the stability and quantum efficiency [34]. Xiao *et al.* applied deuteration in photovoltaic active-layer materials by poly(3-hexylthiophene)/[6,6]-phenyl-C61–butyl methyl ester (PCBM) and selective deuteration of hydrogen on the main and side chains was able to influence the crystalline behavior of the molecule, leading to different photovoltaic properties [35]. In medical applications, deuteration may affect the pharmacokinetic and metabolic properties of drugs and can redirect the metabolic pathway towards reduced toxicity [36]. Rriehna *et al.* illustrated that $CDCl_3$ is less hepatotoxic than $CHCl_3$, suggesting that chloroform hepatotoxicity is related to the metabolic pathway [37]. Hook *et al.* quantitatively investigated the effect of $CDCl_3$ substitution on the nephrotoxicity and hepatotoxicity of $CHCl_3$ in male ICR mice. They quantified the effect of $CDCl_3$ substitution on $CHCl_3$ nephrotoxicity and hepatotoxicity in male ICR mice, and measured renal and hepatic injuries 24 h after administration of different doses of $CHCl_3$ or $CDCl_3$, and proved that the toxicity of $CDCl_3$ to the kidneys was less than that of $CHCl_3$ [38,39]. Combining the above and the market information on the commercial products of deuterium substituting reagents, we found that the use of deuterium chloroform (DC) as a solvent of the process has the following advantages at present: (1) Since DC is a deuterium substitution for chloroform, it also has good solubility for photovoltaic materials; (2) DC is less toxic, less acutely toxic, and less hazardous to the human body; (3) industry of DC is already mature and DC is a commonly used reagent for nuclear magnetic instruments and organic synthesis of raw materials, and also, DC is medicine commonly used as anesthetics; (4) DC is less expensive compared to the UC; (5) small packaged DC products can be purchased in the market, so the use of DC instead of UC can avoid frequent access to the reagents caused by pollution and deterioration. In this work we present the results that DC is an alternative excellent solvent to replace UC for preparation of high-efficient OSCs. First, we based on PM6:BTP-eC9 and used both DC and UC to process the OSC devices. After counting 100 devices for each DC and UC, it is interesting that DC can supply better reproducibility, superior device stability upon storage under the N_2 condition and a little better performance. This is consistent with the slightly increased mobilities and reduced recombination. Second, we again based PM6:Y6 and D18-Cl:Y6 to check the availability of DC for processing the Y6 based and D18-Cl based materials. Positive results were obtained. Third, we again used DC to fabricate OSCs based on several binary and ternary systems. Again, positive results were obtained.

We selected the state-of-the-art PM6:BTP-eC9 binary system and deuterated chloroform as the processing solvent to investigate the effects of both DC and UC on the photovoltaic performance of OSCs. The chemical structures of PM6 and BTP-eC9 are shown in Fig. 1a. The devices were made of indium tin oxide (ITO)/poly(3,4-ethylenedioxythiophene):poly(styrene sulfonate) (PEDOT:PSS)/active layer/PDINO/Al. The weight ratio of the donor to the acceptor was kept at 1.0:1.2 (w/w) and DC was used to dissolve the donor/acceptor materials. As shown in Table 1, when DC was used as the processing solvent, the devices showed a maximum PCE of 16.41% with a V_{OC} of 0.828 V, a J_{SC} of 26.04 mA/cm^2, and a fill factor (FF) of 76.12%. By counting 100 devices, the average PCE is 15.51% ± 0.57% with an average of V_{OC} of 0.825 ± 0.007 V, a J_{SC} of 25.41 ± 0.95 mA/cm^2, and an FF of 74.15% ± 1.75%. When UC was used as the processing solvent, the maximum PCE was 16.38%, the V_{OC} was 0.827 V, the J_{SC} was 25.87 mA/cm^2 and the FF was 76.54%. By counting 100 devices, the average PCE is 15.43% ± 0.58% with an average of V_{OC} of 0.824 ± 0.007 V, a J_{SC} of 25.29 ± 0.97 mA/cm^2, and an FF of 74.19% ± 1.76%. Fig. 1b shows the current density-voltage (*J-V*) characteristics of the OSCs with DC and UC at 100 mW/cm^2 of light. As can be seen from the optimal devices, the devices prepared by DC and UC are similar in terms of PCE. Interestingly, the average PCE of the DC-processed devices is slightly higher than that of the UC-processed ones, mainly due to the slight enhancement of the average J_{SC}, which tentatively suggests that DC can be used as a processing solvent to replace UC.

To explore the reason for the current enhancement, our external quantum efficiency (EQE) curves based on PM6:BTP-eC9 processed with DC and UC, respectively, are shown in Fig. 1c. The maximum EQE is in the wavelength region of 460–820 nm, with a value of 80% for both DC- and UC-treated devices. Compared to the UC-processed device, the DC-processed has a slightly enhanced photon response between 680 nm and 820 nm, contributing to the

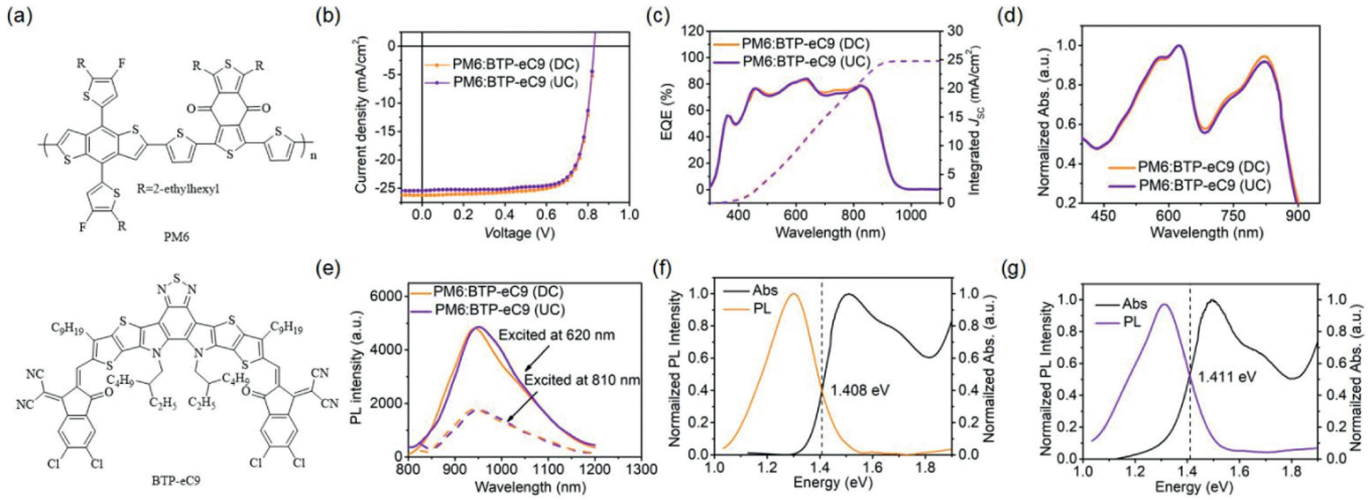

Fig. 1. (a) Chemical structures of PM6 and BTP-eC9. (b) *J-V* characteristics and (c) EQE curves of the best device. (d) Normalized UV–vis absorption spectra of PM6:BTP-eC9 blend films prepared with DC and UC, respectively. (e) PL spectra of PM6:BTP-eC9 blend films prepared with DC and UC, excited at 620 or 810 nm, respectively. Normalized UV–vis absorption and PL spectra of PM6:BTP-eC9 blend films in (f) DC and (g) UC to determine optical bandgap $E_{g,opt}$ from the intersection point of the absorption and PL curves.

Table 1
Summary of device data for PM6:BTP-eC9 fabricated with deuterated chloroform and ultra-dry chloroform, respectively. All data are obtained under the illumination of an AM 1.5G (100 mW/cm^2) light source.

Solvent	V_{OC} [a] (V)	J_{SC} [a] (mA/cm^2)	J_{cal} [b] (mA/cm^2)	FF [a] (%)	PCE [a] (%)
DC	0.828 (0.825 ± 0.007)	26.04 (25.41 ± 0.95)	24.85	76.12 (74.15 ± 1.75)	16.41 (15.51 ± 0.57)
UC	0.827 (0.824 ± 0.007)	25.87 (25.29 ± 0.97)	24.76	76.54 (74.19 ± 1.76)	16.38 (15.43 ± 0.58)

[a] Average values from 100 devices are shown in parentheses.
[b] Calculated from the EQE spectrum.

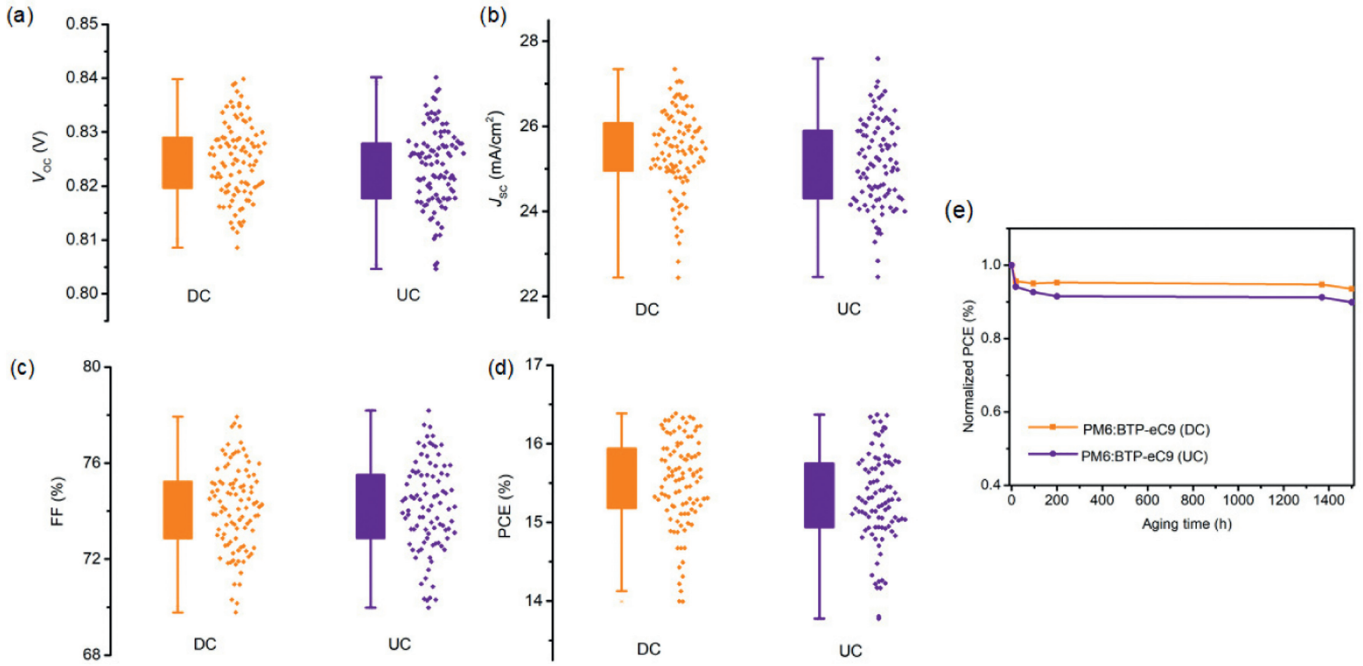

Fig. 2. (a) V_{OC} box plot, (b) J_{SC} box plot, (c) FF box plot, and (d) PCE box plot of PM6:BTP-eC9 based devices prepared with DC and UC, respectively. The data were counted from 100 devices. (e) Aging test chart of the DC- and UC-processed PM6:BTP-eC9 based devices.

enhancement of J_{SC}. The integration currents of the EQE curves are 24.85 and 24.76 mA/cm^2, respectively, which are in agreement with the J_{SC} obtained from *J-V* measurements within 3% error.

As shown in Fig. 1d, we tested the UV–vis absorption spectra of PM6:BTP-eC9 blend films prepared with DC and UC, respectively. The two absorption peaks at 624 nm and 819 nm corresponded to the maximum absorption peaks of PM6 and BTP-eC9, respectively. Compared with the UC-processed samples, the DC-processed samples showed enhanced absorption at 680–820 nm, which coincides with the enhancement of EQE response in this wavelength region. This explains the slightly higher current of the DC-prepared device than the UC-prepared device. Fig. 1e shows the photoluminescence (PL) profiles of PM6:BTP-eC9 blend films spin-coated from DC and UC solutions, respectively. It can be seen that both samples showed nearly identical PL profiles. Compared with the PL obtained from the UC film, the PL of the DC film is slightly blue-shifted. This plus the absorption enhancement observed in 680–820 nm suggests that the use of DC as the processing solvent may slightly tune the aggregation of BTP-eC9 molecules in difference with the use of UC. The optical band gaps of PM6:BTP-eC9 blend films processed with DC and UC were calculated from Figs. 1f and g. They are similar for each other with $E_{g,opt,DC} = 1.408$ eV and $E_{g,opt,UC} = 1.411$ eV. The similar optical band gaps and again the similar V_{OC} values obtained with the DC and UC as the processing solvents suggest that the V_{loss}s of the DC- and UC-prepared devices are also similar, and that DC can be used as an alternative solvent to replace UC. Next, we produced boxplots of each parameter of the PM6:BTP-eC9 devices by counting from 100 devices, as shown in Figs. 2a-d. Compared with the UC-processed devices, the J_{SC} distribution range of the DC-processed devices is found to be more concentrated, which indicates that the J_{SC} reproducibility of the DC-processed devices is better. The mean values of J_{SC}, V_{OC}, and PCE for the DC-processed devices are slightly higher than those for the UC-processed ones. The FF values are however slightly lower than those from the UC-prepared devices. Overall, the boxplot trend of DC devices is more stable, which means that DC might be a more suitable solvent than UC for application in production of OSCs. As shown in Fig. 2e and Table S1 (Supporting information), the un-encapsulated DC devices showed better storage stability under the N_2 atmosphere at 25 ± 5 °C than the UC devices. The DC devices maintained 93.5% of the initial PCE after 200 h, while the UC devices retained 89.9% of the initial PCE after 1500 h.

The charge transport characteristics of the devices were studied using the space charge limiting current (SCLC) method. The electron (μ_e) and hole (μ_h) mobilities were measured separately using the electron-only ITO/TIPD/active layer/PDINO/Al (800 nm) and hole-only (ITO/PEDOT:PSS/active layer/Ag) devices. The data were shown in Figs. S1a and b and Table S2 (Supporting information), the μ_h and μ_e values for the DC-prepared devices were $4.17/3.62 \times 10^{-4}$ cm^2 V^{-1} s^{-1}, and those for the UC-prepared devices were $4.12/3.58 \times 10^{-4}$ cm^2 V^{-1} s^{-1}. The slightly elevated mobilities of the DC device consistent with a slightly higher J_{SC}. The dependence of J_{SC} and V_{OC} on light intensity (P_{light}) was measured to study the charge recombination of the DC- and UC-prepared devices. $J_{SC} \propto P^{\alpha}$ was used to describe the relationship between J_{SC} and light intensity (Fig. S1c in Supporting information). For devices prepared with DC and UC as processing solvents, the α values were

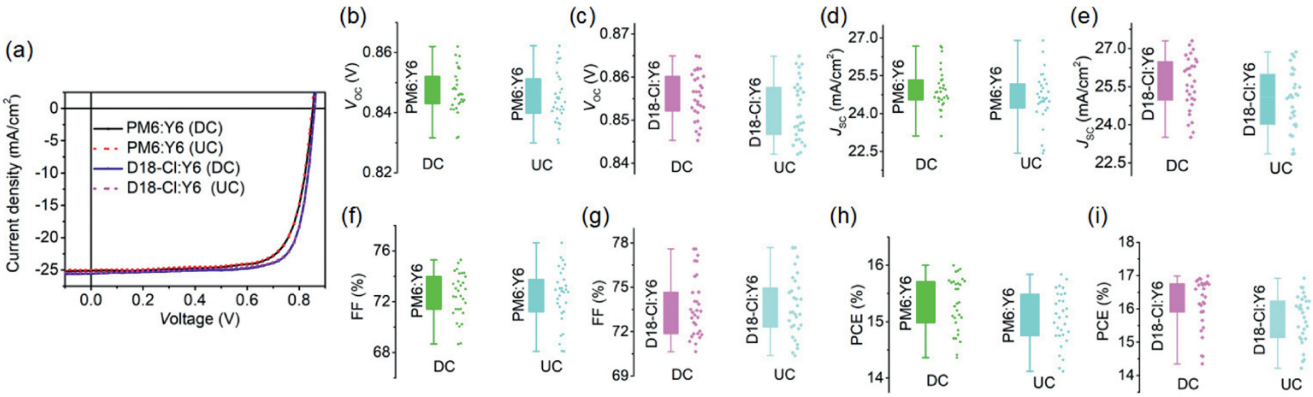

Fig. 3. *J-V* characteristics (a), V_{OC} box plots (b, c), J_{SC} box plots (d, e), FF box plots (f, g), and PCE box plots (h, i) of the PM6:Y6 and D18-Cl:Y6 based binary devices with DC and UC as the processing solvent, respectively.

0.967 and 0.968 (Fig. S1c). The similar α values show that the degree of inhibition of bimolecular complexation is similar for the two devices. The study of trap-assisted recombination can be estimated based on the relationship between $V_{OC} \propto n(kT/q)\ln(P_{light})$, as shown in Fig. S1d (Supporting information). In this equation, *K*, *T*, and *q* represent the Boltzmann constant, temperature, and elementary charge, respectively. The values of *n* for the devices prepared with DC and UC as processing solvents are 1.277 and 1.282, respectively. The similar *n* values indicate that the trap-assisted recombination in the DC devices is similar to that in the UC devices.

To study the charge dissociation and collection in the devices, the relationship curves between the photocurrent density (J_{Ph}) and the effective voltage (V_{eff}) were plotted as a way to calculate the exciton dissociation (η_{diss}) and charge collection efficiency (η_{coll}). Here, J_{ph} is calculated by the equation $J_{ph} = J_L - J_D$, where J_L and J_D are calculated from the current densities under light and dark conditions, respectively. $V_{eff} = V_{Bi} - V_{bias}$, where V_{Bi} is the voltage when $J_{Ph} = 0$ and V_{bias} is the applied bias voltage. As shown in Fig. S1e (Supporting information), J_{sat} is the saturated photocurrent density value. η_{diss} and η_{coll} can be estimated based on $J_{ph,sc}/J_{ph,sat}$ ($J_{ph,sc}$ is the photocurrent densities under short-circuited conditions) and $J_{ph,mmp}/J_{ph,sat}$ ($J_{ph,mmp}$ is the photocurrent densities at the maximum power output conditions), respectively. The η_{diss} value (95.7% *vs.* 95.9%) and η_{coll} value (83.6% *vs.* 83.7%) of the DC devices are close to the UC-prepared devices.

To showcase the versatility of DC in other systems, we validated its use in two additional classical systems: PM6:Y6 and D18-Cl:Y6. Fig. 3a shows the *J-V* characteristics of the two binaries-based devices. Table S3 (Supporting information) lists the photovoltaic performance and Figs. 3b-i demonstrate the distributions of parameters obtained from the two processing solvents. We can see from Table S3 and Figs. 3b-i that the binary devices' performance based on PM6:Y6 and D18-Cl:Y6 exhibit a similar trend to the PM6:BTP-eC9 system, *i.e.* the DC processed device had a more concentrated distribution of J_{SC}s, better reproducibility, and slightly higher V_{OC}s and PCEs compared to the devices prepared with UC as the solvent. For the PM6:Y6 system, the J_{SC} value has a higher value and a narrower distribution (24.87 ± 0.79 mA/cm^2 *vs.* 24.79 ± 0.91 mA/cm^2), showing better reproducibility. Additionally, the PCE value (15.21% *vs.* 15.19%) is slightly higher than those prepared using UC. These results are averaged over 30 cell samples. The J_{SC} values of the D18-Cl:Y6 system were higher and more reproducible (25.61 ± 1.06 mA/cm^2 *vs.* 25.21 ± 1.08 mA/cm^2). Additionally, the V_{OC} values (0.856 ± 0.05 V *vs.* 0.854 ± 0.009 V) and PCE values (16.18% ± 0.76% *vs.* 15.94% ± 0.75%) were slightly higher than those of the UC-processed devices.

To further prove the general applicability of DC used to prepare highly efficient OSC devices, we selected PM6:L8-BO, PM6:BTP-BO-4F and J71:IDIC as well as PM6:L8-BO:IDIC to fabricate the OSC devices with DC as the processing solvent. The photovoltaic data was shown in Table S4 (Supporting information) and the *J-V* and EQE data were given in Figs. S2a-d (Supporting information). All of them showed expected photovoltaic performance. The integrated short-circuit current-density values from the EQE spectra are coincided with the values from the *J-V* measurements within 3% of the errors. The PCE of the PM6:L8-BO blend is 16.73%, the PCE of the PM6:BTP-BO-4F blend is 14.64%, the PCE of the J71:IDIC blend is 10.70%, and the PCE of PM6: IDIC:L8-BO blend is 17.14%. These values coincided with the values reported in the literature [40–45].

In all, our results clearly indicate that DC is a viable alternative to UC for the use in the field of OSCs and enable to stably reproduce high-efficient OSC devices with more reproducibility and slightly more efficiencies.

In summary, we have presented a strategy for the preparations of the active layers of OSCs using DC as the processing solvent, which has the following advantages over the UC: (1) DC has a good solubility for photovoltaic materials, and the devices prepared by DC as a solvent are comparable to those prepared by UC as the solvent in terms of performance, and can maintain the solar cell efficiency with slighter improvement. (2) The DC used in this strategy is weaker toxic and less acutely toxic compared to UC, which is less potentially threatening to the human body and enhances market competitiveness. (3) The DC used in this strategy is mature in its industrial preparation, and there are small packaged products in the market, that can avoid reagent contamination and deterioration caused by frequent access to reagents, and the cost of DC is lower compared to UC. (4) The performance of OSCs prepared by DC is highly reproducible in term of J_{SC}, and the average values of V_{OC} and PCE are slightly higher than those of the devices prepared by UC. (5) The stability of the devices fabricated with DC is better. (6) Using DC as a processing solvent is suitable for a variety of OSC material systems.

In conclusion, this work proves that DC can replace UC as a processing solvent for the preparation of organic solar cells, which enhances the market competitiveness in organic solar cells for laboratory preparation and future commercialization.

Declaration of competing interest

The authors declare that they have no known competing financial interests or personal relationships that could have appeared to influence the work reported in this paper.

CRediT authorship contribution statement

Zhiyang Zhang: Writing – original draft, Investigation, Formal analysis, Data curation. **Yi Chen:** Methodology, Formal analysis, Data curation. **Yingnan Zhang:** Data curation. **Chuanlang Zhan:** Writing – review & editing, Visualization, Supervision, Project administration, Methodology, Funding acquisition, Conceptualization.

Acknowledgments

The authors acknowledge the financial supports from the Department of Science and Technology of Inner Mongolia Autonomous Region (No. 2020GG0192), the Natural Science Foundation of Inner Mongolia Autonomous Region (No. 2022ZD04), and Inner Mongolia Normal University.

Supplementary materials

Supplementary material associated with this article can be found, in the online version, at doi:10.1016/j.cclet.2024.110083.

References

[1] H. Sun, P.Y. Zhang, Y.N. Zhang, C.L. Zhan, Chem. J. Chin. Univ. 44 (2023) 20230076.
[2] Y. Wang, Q. Chen, S. Liang, et al., Chin. Chem. Lett. 35 (2024) 109164.
[3] W. Feng, T. Chen, Y. Li, et al., Angew. Chem. Int. Ed. 63 (2024) e202316698.
[4] C. He, Q. Shen, B. Wu, et al., Adv. Energy Mater. 13 (2023) 2204154.
[5] G. Cai, Z. Chen, T. Li, et al., J. Mater. Chem. A 10 (2022) 21061–21071.
[6] Y. Li, Y. Cai, Y. Xie, et al., Energy Environ. Sci. 14 (2021) 5009–5016.
[7] T. Huang, Z. Zhang, Q. Liao, et al., Small 19 (2023) 2303399.
[8] B. Pang, C. Liao, X. Xu, et al., Adv. Mater. 35 (2023) 2300631.
[9] L. Zhan, S. Li, Y. Li, et al., Adv. Energy Mater. 12 (2022) 2201076.
[10] M. Deng, X. Xu, Y. Duan, et al., Adv. Mater. 35 (2023) 2210760.
[11] J. Gao, X. Zhu, H. Bao, et al., Chin. Chem. Lett. 34 (2023) 107968.
[12] J. Wang, Y. Wang, P. Bi, et al., Adv. Mater. 35 (2023) 2301583.
[13] J. Song, C. Zhang, C. Li, et al., Angew. Chem. Int. Ed. 63 (2024) e202404297.
[14] S. Luo, C. Li, J. Zhang, et al., Nat. Commun. 14 (2023) 6964.
[15] T. Chen, S. Li, Y. Li, et al., Adv. Mater. 35 (2023) 2300400.
[16] K. Chong, X. Xu, H. Meng, et al., Adv. Mater. 34 (2022) 2109516.
[17] Z. Zheng, J. Wang, P. Bi, et al., Joule 6 (2022) 171–184.
[18] F. Zhao, C. Wang, X. Zhan, Adv. Energy Mater. 8 (2018) 1703147.
[19] G. Zhang, F.R. Lin, F. Qi, et al., Chem. Rev. 122 (2022) 14180–14274.
[20] L. Zhu, M. Zhang, W. Zhong, et al., Energy Environ. Sci. 14 (2021) 4341–4357.
[21] W. Chen, T. Xu, F. He, et al., Nano Lett. 11 (2011) 3707–3713.
[22] S. Guo, E.M. Herzig, A. Naumann, et al., J. Phys. Chem. B 118 (2014) 344–350.
[23] I. Burgués-Ceballos, F. Machui, J. Min, et al., Adv. Funct. Mater. 24 (2014) 1449–1457.
[24] C. McDowell, M. Abdelsamie, M.F. Toney, G.C. Bazan, Adv. Mater. 30 (2018) 1707114.
[25] J. Mao, J. Iocozzia, J. Huang, et al., Energy Environ. Sci. 11 (2018) 772–799.
[26] K. Yang, M. Lv, Y. Chang, K. Lu, Z. Wei, Chin. Chem. Lett. 35 (2024) 109018.
[27] W. Zhang, J. Huang, X. Lv, et al., Chin. Chem. Lett. 34 (2023) 107436.
[28] S.H. Park, A. Roy, S. Beaupré, et al., Nature Photon 3 (2009) 297–302.
[29] H. Tan, W. Zhang, P. Zhang, et al., Solar RRL 6 (2022) 2200147.
[30] P. Ding, D. Yang, S. Yang, Z. Ge, Chem. Soc. Rev. 53 (2024) 2350–2387.
[31] Y. Su, Z. Ding, R. Zhang, et al., Sci. China Chem. 66 (2023) 2380–2388.
[32] Z. Zhang, J. Wang, Z. Hu, et al., Chin. Chem. Lett. 34 (2023) 108527.
[33] P. Zhang, Z. Zhang, H. Sun, et al., Chin. Chem. Lett. 35 (2024) 108802.
[34] C.C. Tong, K.C. Hwang, J. Phys. Chem. C 111 (2007) 3490–3494.
[35] M. Shao, J. Keum, J. Chen, et al., Nat. Commun. 5 (2014) 3180.
[36] E.M. Russak, E.M. Bednarczyk, Ann. Pharmacother. 53 (2019) 211–216.
[37] L.R. Pohl, G. Rriehna, Life Sci. 23 (1978) 1067–1072.
[38] M. Ahmadizadeh, C.H. Kuo, J.B. Hook, J. Toxicol. Environ. Health 8 (1981) 105–111.
[39] L. Li, J. Jakowski, C. Do, K. Hong, Macromolecules 54 (2021) 3555–3584.
[40] A. Wang, Y. Kang, C. Hou, et al., Sci. Bull. 68 (2023) 1153–1161.
[41] M. Deng, X. Xu, Y. Duan, et al., Adv. Funct. Mater. 33 (2023) 2212290.
[42] A. Lan, Y. Lv, J. Zhu, et al., ACS Energy Lett. 7 (2022) 2845–2855.
[43] K. Li, Y. Wu, Y. Tang, et al., Adv. Energy Mater. 9 (2019) 1901728.
[44] X. Li, M.A. Pan, T.K. Lau, et al., Chem. Mater. 32 (2020) 5182–5191.
[45] L. Zhong, H. Bin, Y. Li, et al., J. Mater. Chem. A 6 (2018) 24814–24822.